Short Communication

Suppression of Advanced Human Prostate Tumor Growth in Athymic Mice by Silibinin Feeding Is Associated with Reduced Cell Proliferation, Increased Apoptosis, and Inhibition of Angiogenesis[1]

Rana P. Singh, Girish Sharma, Sivanandhan Dhanalakshmi, Chapla Agarwal, and Rajesh Agarwal[2]

Department of Pharmaceutical Sciences, School of Pharmacy [R. P. S., G. S., S. D., C. A., R. A.], University of Colorado Cancer Center [R. A.], University of Colorado Health Sciences Center, Denver, Colorado 80262

Abstract

Recently, we observed that dietary feeding of silibinin strongly prevents and inhibits the growth of advanced human prostate tumor xenografts in athymic nude mice without any apparent signs of toxicity together with increased secretion of insulin-like growth factor-binding protein 3 from the tumor in to mouse plasma (R. P. Singh *et al.*, Cancer Res., *62:* 3063–3069, 2002). In the present study, we investigated the effect of silibinin feeding [0.05% and 0.1% (w/w) in diet for 60 days] on the prognostic biomarkers (namely, proliferation, apoptosis, and angiogenesis) in the prostate tumor xenografts of the above-reported study. Immunohistochemical analysis of the tumors for proliferating cell nuclear antigen and Ki-67 showed that silibinin decreases proliferation index by 28–60% and 30–60% ($P < 0.001$) as compared with their controls, respectively. *In situ* detection of apoptosis by terminal deoxynucleotidyl transferase dUTP-mediated nick end labeling staining of tumors showed a 7.4–8.1-fold ($P < 0.001$) increase in apoptotic cells in silibinin-fed groups over that of control group. Silibinin also increased activated caspase 3-positive cells by 2.3–3.6-fold ($P < 0.001$). CD31 staining for tumor vasculature showed a significant decrease (21–38%; $P < 0.001$) in tumor microvessel density in silibinin-fed groups of tumors as compared with control group of tumors. Tumor sections were also analyzed for vascular endothelial growth factor and insulin-like growth factor-binding protein 3 protein expression, and a slightly decreased and a moderately increased cytoplasmic immunostaining in silibinin-fed groups were observed as compared with the control group, respectively. Together, these results suggest that inhibition of advanced human prostate tumor xenograft growth in athymic nude mice by silibinin is associated with its *in vivo* antiproliferative, proapoptotic, and antiangiogenic efficacy in prostate tumor.

Introduction

Epidemiological studies followed by laboratory studies and *vice versa* have shown that dietary agents are one of the important factors in reducing cancer risk, as the differences in worldwide human cancer incidence and mortality often depend on lifestyle and dietary habits (1–3). There are several reports in which diets rich in naturally occurring polyphenolic flavonoid antioxidants have been shown to be associated with the reduced incidence of various human cancers (1–5). Silymarin belongs to one of these flavonoids, which is isolated from milk thistle (*Silybum marianum*) L. Gaertn (6). It is already in clinical use for its antihepatotoxic properties in Europe and Asia and has also recently been marketed in the United States and Europe as a dietary supplement (6, 7). Silibinin, a flavanone, is the major bioactive component present in silymarin. The recent studies showed that silymarin/silibinin is effective in treating a wide range of liver and gall bladder diseases, including hepatitis and cirrhosis as well as dermatological conditions (7, 8). Nontoxicity is one of the most important properties of this compound, which has been tested in various animal models using different modes of administration; surprisingly, there is no known LD_{50} in laboratory animals (7, 8). In humans, adverse effects of silymarin/silibinin therapy are very rare and are limited to nausea, headache, arthralgia (joint pain), pruritus (itching), urticaria (temporary skin swelling), and mild laxative (reviewed in Ref. 8). Several studies in rodents and cell cultures by others and us have shown that silymarin/silibinin provides significant protection against different cancers of epithelial origin including PCA[3] (9–13).

Several epigenetic alterations leading to constitutively active mitogenic and cell survival signaling, as well as loss of apoptotic response, are causally involved in uncontrolled growth of PCA, leading to androgen-independent growth, apoptosis resistance, and increased expression and secretion of angiogenic factors (14, 15). Therefore, one targeted approach for PCA prevention, growth control, and/or treatment could be

[3] The abbreviations used are: PCA, prostate cancer; IGF, insulin-like growth factor; IGFBP-3, insulin-like growth factor-binding protein 3; PCNA, proliferating cell nuclear antigen; TUNEL, terminal deoxynucleotidyl transferase dUTP-mediated nick end labeling; VEGF, vascular endothelial growth factor; DAB, 3,3′-diaminobenzidine; TdT, terminal deoxynucleotidyl transferase.

the inhibition of molecular events involved in PCA growth, progression, and angiogenesis. In this regard, our extensive studies with silibinin and silymarin in PCA cells have shown that these agents exert pleiotropic anticancer effects in cell culture studies. Our mechanistic studies showed that silibinin/silymarin alters cell cycle progression and inhibits mitogenic and cell survival signaling involving epidermal growth factor receptor, IGF-I receptor, and nuclear factor κB in PCA cells (16–18). We also observed that silymarin inhibits the secretion of VEGF from PCA cells and causes growth inhibition and apoptotic death of human umbilical vein endothelial cells accompanied by disruption of capillary tube formation on Matrigel (19). Our most recently completed study showed that dietary feeding of silibinin inhibits advanced human prostate carcinoma DU145 tumor xenograft growth in athymic nude mice (13). In the present study, we investigated the *in vivo* effect of dietary feeding of silibinin on cell proliferation, apoptosis, and angiogenesis as well as VEGF and IGFBP-3 protein levels in DU145 tumor xenografts.

Materials and Methods

Research Strategy and Study Samples. Our strategy was to investigate the biomarkers associated with the growth-inhibitory effect of silibinin on prostate tumor xenografts. As mentioned earlier, we recently observed that dietary feeding of silibinin strongly inhibits the growth of advanced human prostate DU145 tumor xenografts in athymic nude mice without any apparent signs of toxicity (13). In the present study, we took these DU145 prostate tumor samples from the tumor xenograft experiment in which mice were fed with control and silibinin [0.05% and 0.1% silibinin (w/w) in AIN-93M purified] diets for 60 days, showing 35–58% ($P < 0.05$–0.001) decrease in tumor volume/tumor in silibinin-fed mice at the end of the study. In this study, we also observed that silibinin significantly increases (up to ~6-fold, $P < 0.05$) tumor-secreted human IGFBP-3 levels in mouse plasma. These tumor samples were used for the immunohistochemical analysis of prognostic biomarkers (namely, proliferation, apoptosis, and angiogenesis) and VEGF and IGFBP-3 protein expression in prostate tumors.

Immunohistochemical Detection of PCNA and Ki-67 in Tumors. Tumor samples were fixed in 10% buffered formalin for 12 h and processed conventionally. The paraffin-embedded tumor sections (5-μm thick) were heat immobilized, deparaffinized using xylene, and rehydrated in a graded series of ethanol with a final wash in distilled water. Antigen retrieval was done in 10 mM citrate buffer (pH 6.0) in a microwave for 2 and 18 min at full and 20% power levels, respectively. Endogenous peroxidase activity was blocked by immersing the sections in 3.0% H_2O_2 in methanol (v/v), followed by three changes in 10 mM PBS (pH 7.4). The sections were then incubated with mouse monoclonal anti-PCNA antibody IgG2a (1:400) or anti-Ki-67 antibody, clone MIB-1 (1:150; Dako, Carpinteria, CA) for 1 h at 37°C in a humidity chamber. Negative controls were treated only with PBS under identical conditions. The sections were then incubated with biotinylated rabbit antimouse antibody IgG (1:200 in 10% normal rabbit serum) for 30 min at room temperature. Thereafter, following wash with PBS, sections were incubated with conjugated horseradish peroxidase streptavidin (Dako) for 30 min at room temperature in a humidity chamber. The sections were then incubated with DAB (Sigma Chemical Co., St. Louis, MO) working solution for 10 min at room temperature, counterstained with diluted Harris hematoxylin (Sigma Chemical Co.) for 2 min, and rinsed in Scott's water. Finally, proliferating cells were

quantified by counting the PCNA-positive cells and the total number of cells at 10 arbitrarily selected fields at ×400 magnification in a double-blinded manner. The proliferation index (per ×400 microscopic field) was determined as number of PCNA- or Ki-67-positive cells × 100/total number of cells.

***In Situ* Apoptosis Detection by TUNEL Staining.** The formalin-fixed and paraffin-embedded 5-μm-thick sections of all tumor samples (those used for PCNA staining) were used to identify early as well as late apoptotic cells by TUNEL staining. DNA fragmentation in individual apoptotic cells was visualized by detection of biotinylated nucleotides incorporated onto the free 3′-hydroxyl residues of these DNA fragments by Tumor TACS *in situ* Apoptosis Detection Kit (R&D Systems, Inc., Minneapolis, MN). Briefly, tumor sections were cleared in xylene and rehydrated in graded concentrations of ethanol. Slides were rinsed with Ca^{2+}, Mg^{2+}, and DNase-free PBS [10 mM PBS (pH 7.4)] and permeabilized with proteinase K at room temperature to make the DNA accessible to the labeling enzyme. For positive control, section was incubated with TACS nuclease for 30 min, which generated DNA strand breaks in virtually every cell. Endogenous peroxidase activity was quenched using 5% H_2O_2 (in methanol, v/v) for 5 min, and sections were incubated with TdT labeling buffer for 5 min before starting the labeling reaction. Then sections were incubated with TdT enzyme and biotinylated nucleotides (for negative control, labeling buffer was used instead of TdT enzyme) for 1 h at 37°C in a humidified chamber. The reaction was stopped by adding TdT stop buffer for 5 min. Sections were incubated with streptavidin-conjugated horseradish peroxidase for 10 min. Brown color was developed with incubation in DAB solution (Sigma) for 7 min at room temperature. The slides were counterstained in 1% methyl green for 1.5 min and visualized and scored under a light microscope. The apoptosis was evaluated by counting the positive cells (brown-stained cells) as well as the total number of cells at 10 arbitrarily selected fields at ×400 magnification in a double-blinded manner. The apoptotic index (per ×400 microscopic field) was calculated as number of apoptotic cells × 100/total number of cells.

Immunohistochemical Detection of Activated Caspase 3. Paraffin-embedded tumor sections were immunohistochemically analyzed for cleaved caspase 3 by following the vendor's protocol supplied with the antibody (catalogue number 9661; Cell Signaling Technology, Inc., Beverly, MA) step by step. The primary antibody used was polyclonal cleaved caspase 3 (Asp-175) in a 1:100 dilution overnight at 4°C. Finally, sections were developed by DAB reagent and counterstained with diluted Harris hematoxylin. Cleaved caspase 3-stained cells (brown) were quantified (number of positive cells × 100/total number of cells) in 10 random microscopic (×400) fields per tumor by an independent observer.

Immunohistochemical Analysis of Tumors for CD31 Expression. Staining procedure for CD31 (an endothelial cell-specific antigen also known as platelet endothelial cell adhesion marker 1) was similar to that of PCNA staining using specific antibody for CD31. Briefly, paraffin-embedded tumor sections were incubated overnight with goat antimouse CD31 polyclonal antibody (Santa Cruz Biotechnology, Santa Cruz, CA) in PBS containing 10% rabbit serum (1:200). Then sections were incubated with biotinylated rabbit antigoat secondary antibody (Santa Cruz Biotechnology) followed by streptavidin-conjugated horseradish peroxidase (Dako). Antigen-antibody complexes were visualized by incubation with DAB substrate and counterstained with diluted Harris hematoxylin. Microvessels

stained with CD31 (brown) were quantified in 10 random microscopic (×400) fields per tumor by an independent observer.

Immunohistochemical Analysis of Tumors for VEGF and IGFBP-3 Protein Expression. Staining procedure for VEGF and IGFBP-3 was similar to that of PCNA staining using specific primary antibodies. Briefly, paraffin-embedded tumor sections were incubated overnight with human reactive rabbit anti-VEGF (1:200) and goat anti-IGFBP-3 (1:200) primary antibodies (Santa Cruz Biotechnology, San Diego, CA) followed by incubation with appropriate biotinylated secondary antibodies. Finally, antigen-antibody complexes were visualized by peroxidase reaction with DAB substrate and counterstained with diluted Harris hematoxylin. Sections were viewed and analyzed by microscope under low (×100) and high (×400) magnifications in a double-blinded manner.

Immunohistochemical and Statistical Analyses. All of the microscopic immunohistochemical analyses were done by Zeiss Axioscop 2 microscope (Carl Zeiss Inc.). Colored images were taken with a Kodak DC290 zoom digital camera. Microscopic images were transferred and processed by Windows Millennium DC290 Kodak microscopy documentation system (Eastman Kodak, New Haven, CT). Mean and SE were used to describe the quantitative data. The statistical significance of difference between control and silibinin-fed groups was determined by ANOVA followed by Tukey test for multiple comparisons. Student's two-tailed t test was used as needed, and P was considered significant at $P < 0.05$. The level of statistical significance was confirmed by the Mann-Whitney U test.

Results

Antiproliferative Effect of Silibinin Feeding in Advanced Human Prostate Tumor Xenograft in Athymic Nude Mice. To assess the *in vivo* effect of silibinin feeding to mice on its antiproliferative responses toward the inhibition of tumor xenograft growth in athymic mice, the tumor samples were analyzed by PCNA and Ki-67 immunostaining. Qualitative microscopic examination of PCNA- and Ki-67-stained tumor sections showed a substantial decrease in PCNA- and Ki-67-positive cells in silibinin-fed groups of tumors as compared with control group tumors (Fig. 1, $A-C$ and $E-G$). The quantification of PCNA immunohistochemical staining showed $34.2 \pm 0.58\%$ and $19.2 \pm 0.20\%$ PCNA-positive cells in silibinin-fed groups of tumors [0.05% and 0.1% (w/w) in diet] as compared with $47.6 \pm 1.28\%$ PCNA-positive cells in controls, respectively (Fig. 1D). Similarly, the quantification of Ki-67 immunohistochemical staining showed $31.6 \pm 1.9\%$ and $17.8 \pm 3.7\%$ Ki-67-positive cells in silibinin-fed groups of tumors [0.05% and 0.1% (w/w) in diet] as compared with control showing $44.72 \pm 1.46\%$ Ki-67-positive cells, respectively (Fig. 1H). In both PCNA and Ki-67 analysis, the decrease in proliferation index in silibinin-fed groups was 28–30% ($P < 0.001$) at the lower dose of silibinin and 60% ($P < 0.001$) at the higher dose of silibinin as compared with control (Fig. 1, D and H). The negative controls, in which PBS was used instead of PCNA or Ki-67 antibody, did not show any considerable positive staining (data not shown).

Apoptotic Effect of Silibinin in Prostate Tumors. *In vivo* apoptotic response of silibinin feeding on prostate tumor was investigated by TUNEL staining. Microscopic examination of the tumor sections showed that, compared with control, silibinin increases the number of TUNEL-positive cells (Fig. 2, $A-C$). The quantitative evaluation of apoptosis showed that silibinin [0.05% and 0.1% (w/w) in diet] causes $18.5 \pm 1.23\%$

and $20.32 \pm 1.81\%$ apoptotic cells as compared with control showing $2.51 \pm 0.39\%$ apoptotic cells, which accounted for a 7.4-fold increase ($P < 0.001$) and an 8.1-fold increase ($P < 0.001$), respectively, over that of control (Fig. 2D). The positive control, in which TACS nuclease was used to generate DNA fragments with free 3′-OH end, showed positive staining in all of the nuclei, whereas the negative control, in which labeling buffer was used instead of TdT, did not show any considerable positive staining (data not shown).
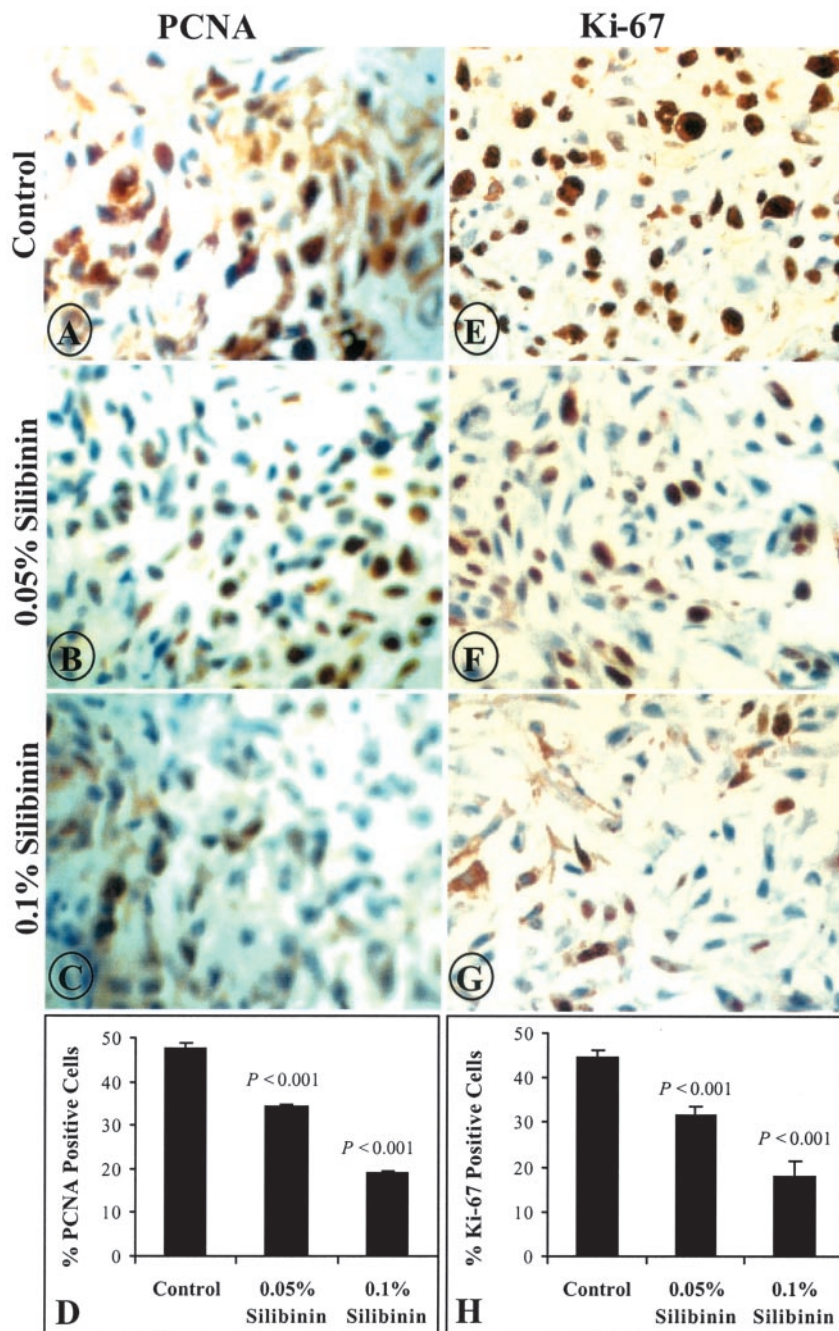
Apoptotic effect of silibinin in prostate tumors was further confirmed by activated caspase-3 immunostaining. Microscopic examination of stained sections showed an increase in cleaved caspase 3-positive cells in silibinin-treated groups as compared with control group (Fig. 2, $E-G$). Quantitative analysis of these sections showed 2.0% and 3.1% cleaved caspase 3-positive cells (in 0.05% and 0.1% silibinin groups, respectively) as compared with 0.87% in control (Fig. 2H). The trend in silibinin-caused increase in activated caspase 3 (2.3–3.6-fold) was quite similar to that of the TUNEL staining data, although it was less in terms of quantitative immunostaining. This could be explained by the fact that caspase activation is an upstream event in apoptosis and could amplify the downstream signal leading to apoptotic death of the cell, and on the other hand, apart from the second executioner caspase 7, there might be caspase 3-independent mechanism(s) involved in the apoptotic effect of silibinin.

Silibinin Inhibits Microvessel Density in Prostate Tumors. The growth and progression of cancers from latent and localized focal carcinomas to invasive carcinomas is dependent on angiogenesis. Tumor microvessel is regarded as an important prognostic marker and an independent predictor of pathological stages and malignant potential of PCA (20). To examine whether strong inhibition of prostate tumor growth by silibinin is accompanied by its *in vivo* antiangiogenic effect, we investigated intratumoral microvessel density by immunohistochemical analysis of endothelial cell-specific marker CD31 (platelet endothelial cell adhesion marker 1). The microscopic examination of tumors after immunohistochemical staining showed numerous cells positive for the expression of CD31 in control group of tumors but showed only sporadic positive cells in the tumors derived from the silibinin-fed group of mice (Fig. 3, $A-C$). We also observed more dilated vessels in control group of tumors as compared with silibinin-fed groups of tumors. Quantification of microvessels showed 14.8 ± 1.0 microvessels/×400 field in control tumors as compared with 11.7 ± 0.24 and 9.1 ± 0.22 microvessels in 0.05% and 0.1% silibinin-diet fed groups of prostate tumors, respectively (Fig. 3D). The decrease in microvessel density in silibinin-diet fed groups was 21% ($P < 0.001$) and 38% ($P < 0.001$) over that of control group, respectively.

Silibinin Moderately Alters VEGF and IGFBP-3 Immunoreactivities in Prostate Tumors. It has been also shown that tumor cells produce and secrete VEGF, a potent and strong mitogen for endothelial cells, for neovascularization of the tumor. Our earlier cell culture study showed that silymarin strongly inhibits VEGF secretion from DU145 cells but not the cellular level of VEGF (19). We recently observed that silibinin increases IGFBP-3 secretion from DU145 tumor xenograft into the mouse plasma (13). Therefore, to assess the *in vivo* effect of silibinin feeding on VEGF and IGFBP-3 protein levels in DU145 prostate tumor xenograft, paraffin-embedded sections of the tumor samples were analyzed by immunohistochemical staining for VEGF and IGFBP-3 using specific antibodies. Microscopic exam-

Fig. 1. *In vivo* antiproliferative effect of dietary feeding of silibinin in human prostate tumor xenograft in athymic nude mice. At the end of the study detailed in "Material and Methods," tumors were excised and processed for immunohistochemical staining for $(A-C)$ PCNA and $(E-G)$ Ki-67. Immunohistochemical analysis was based on DAB staining as detailed in "Materials and Methods." *Top panels,* control; *middle panels,* 0.05% silibinin (w/w) in diet for 60 days; *bottom panels,* 0.1% silibinin (w/w) in diet for 60 days. Quantification of (D) PCNA-positive cells and (H) Ki-67-positive cells for proliferation index. Proliferation index was calculated as the number of positive cells $\times$ 100/total number of cells counted under $\times$400 magnification in 10 randomly selected areas in each tumor sample. The data shown are the mean $\pm$ SE of five samples from an individual mouse in each group. The pictures shown are at $\times$400.

ination of VEGF-stained tumor sections showed a slight decrease in the intensity of VEGF-positive cytoplasmic staining in silibinin-fed groups of tumors as compared with control group tumors (Fig. 3, $E-G$). Similarly, immunohistochemical analysis of tumor sections by IGFBP-3 staining showed a moderate increase in IGFBP-3-positive cytoplasmic staining in silibinin-fed groups of tumors as compared with control group tumors (Fig. 3, $H-J$). These results were evident in about 50% of the 10 randomly selected areas viewed under the microscope ($\times$400) in 60–80% of the tumors examined in the study.

Discussion

The present study provides *in vivo* evidence of the efficacy of silibinin against advanced human PCA growth in nude mice on the basis of immunohistochemical analysis of common biomarkers of cancer therapy in preclinical studies. The end point biomarkers studied were cell proliferation, apoptosis, and tumor angiogenesis. The outcomes of the present investigation showed that dietary feeding of silibinin causing inhibition of advanced human PCA growth in nude mice is associated with a strong and significant decrease in tumor cell proliferation, an increase in apoptosis, and a decrease in tumor microvessel

TUNEL

Activated Caspase 3

Fig. 2. In vivo apoptotic effect of dietary feeding of silibinin in human prostate tumor xenograft in athymic nude mice. At the end of the study detailed in "Material and Methods," tumors were excised and processed for immunohistochemical staining for (*A−C*) TUNEL and (*E−G*) activated caspase 3. Immunohistochemical analysis was based on DAB staining as detailed in "Materials and Methods." *Top panels,* control; *middle panels,* 0.05% silibinin (w/w) in diet for 60 days; *bottom panels,* 0.1% silibinin (w/w) in diet for 60 days. (*D*) Apoptotic index (TUNEL) and (*H*) activated caspase 3 staining were quantified as the number of positive cells × 100/total number of cells counted under ×400 magnification in 10 randomly selected areas in each tumor sample. The data shown are the mean ± SE of five samples from an individual mouse in each group. The pictures shown are at ×400.
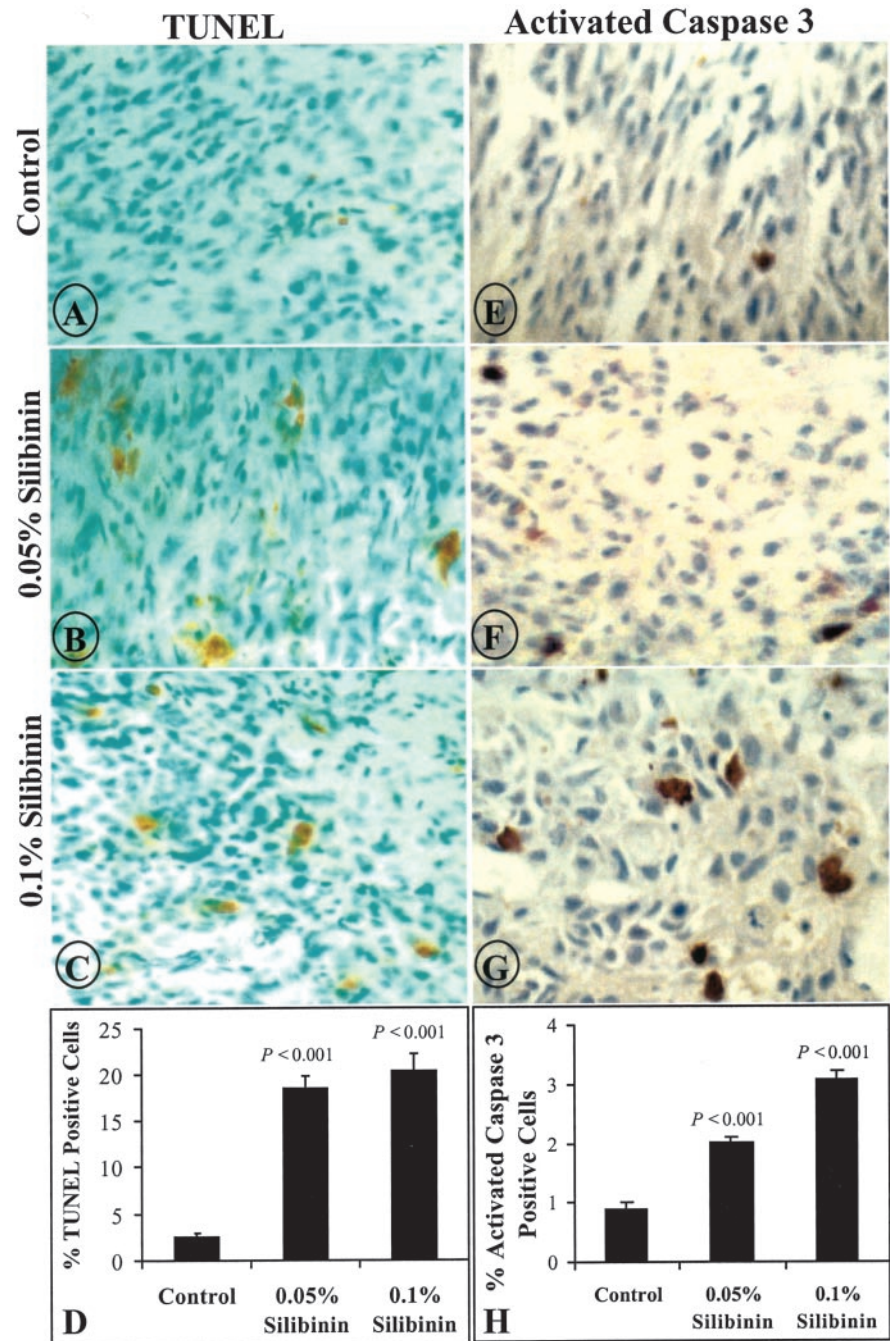
density. Further investigation by immunohistochemical staining of tumor sections showed a slight decrease in VEGF and a moderate increase in IGFBP-3 cytoplasmic staining in silibinin-fed groups of tumors.

Overall, these findings translate the pleiotropic anticancer effects of silibinin in human PCA cell culture studies in to an *in vivo* preclinical PCA model, although mechanistic details of its *in vivo* efficacy remain to be studied. Our present data of PCNA and Ki-67 immunostaining show that silibinin has a strong and significant *in vivo* antiproliferative effect against PCA growth that might involve the inhibition of one or more mitogenic pathway(s), as we observed in cell culture studies

(16–18). Recent epidemiological studies have shown a close association between increasing plasma level of IGF-I and PCA risk, as well as an inverse association with plasma IGFBP-3 levels (21, 22). The observation that silibinin caused a moderate increase in IGFBP-3 immunostaining in tumor xenograft in the present investigation, together with a significant increase (up to ∼6-fold) in its secretion from tumor cells into mouse plasma as reported earlier (13), suggests that up-regulation of IGFBP-3 by silibinin and specifically its enhanced secreted levels in blood circulation might have an inhibitory effect on the mitogenic action of IGF-I in PCA xenograft. It has been reported that apart from antagonizing the mitogenic activity of IGF-I, IGFBP-3
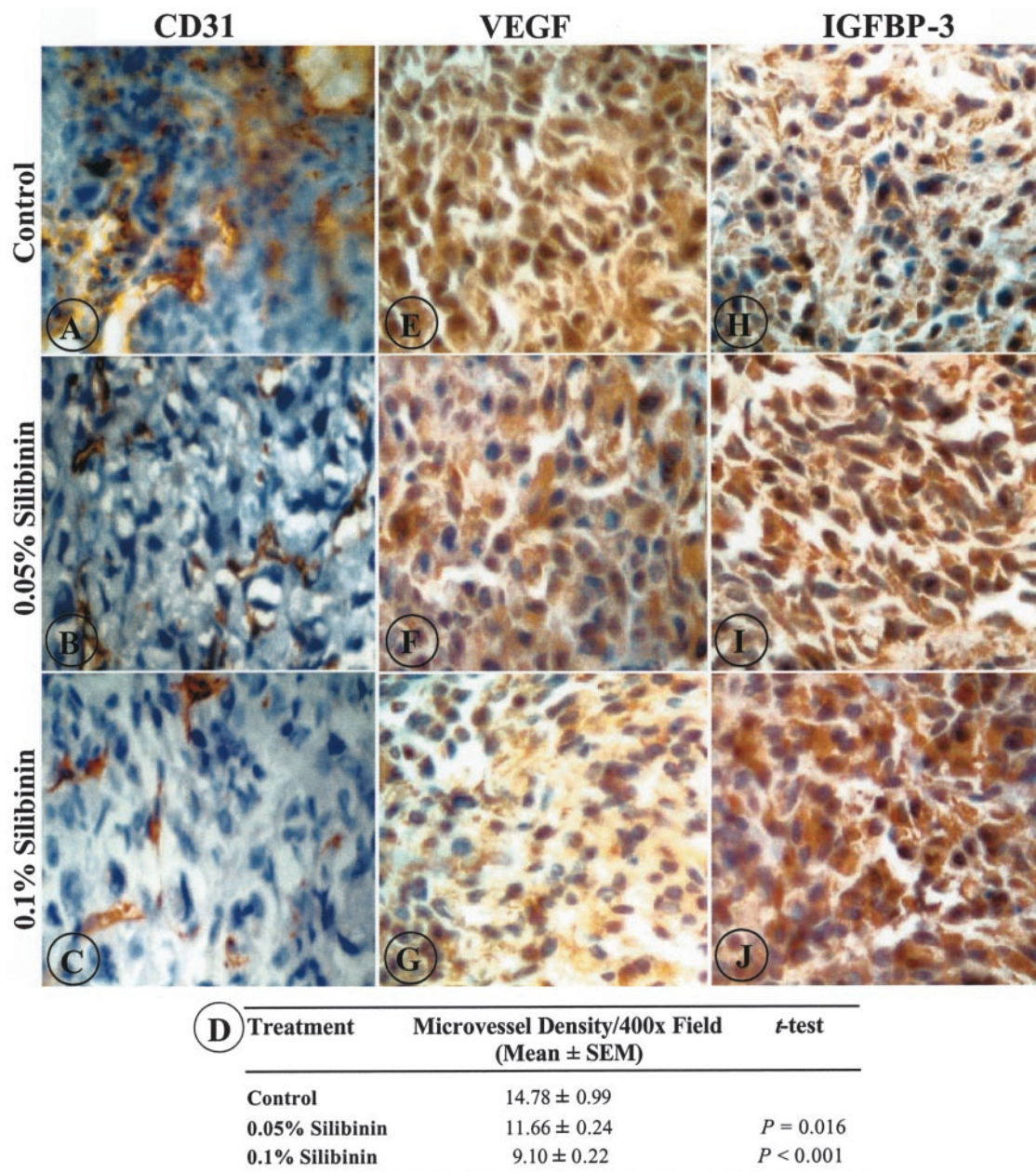
CD31   **VEGF**   **IGFBP-3**

D	Treatment	Microvessel Density/400x Field (Mean ± SEM)	*t*-test
	Control	14.78 ± 0.99	
	0.05% Silibinin	11.66 ± 0.24	$P = 0.016$
	0.1% Silibinin	9.10 ± 0.22	$P < 0.001$

Fig. 3. *In vivo* effects of dietary feeding of silibinin on microvessel density, VEGF, and IGFBP-3 expression in human prostate tumor xenograft in athymic nude mice. At the end of the study detailed in "Material and Methods," tumors were excised and processed for immunohistochemical staining for (*A–C*) endothelial cell-specific antigen CD31, (*E–G*) VEGF, and (*H–J*) IGFBP-3. Immunohistochemical analysis was based on DAB staining as detailed in "Materials and Methods." *Top panels,* control; *middle panels,* 0.05% silibinin (w/w) in diet for 60 days; *bottom panels,* 0.1% silibinin (w/w) in diet for 60 days. (*D*) *In vivo* antiangiogenic effect of silibinin was assessed by counting intratumoral microvessels (CD31-positive staining) under ×400 magnification of microscopic field in 10 randomly selected areas in each tumor sample. The data shown are the mean ± SE of five samples from an individual mouse in each group. The pictures shown are at ×400.

also has IGF-I-independent apoptotic and antiproliferative effects (23). We have observed that silymarin/silibinin causes strong apoptotic death of endothelial cells in culture (19).[4] Therefore, the *in vivo* apoptotic effect of silibinin in prostate tumor xenografts was expected, as we observed in the present study. Furthermore, an increase in activated caspase 3-positive

cells in silibinin-fed tumors indicates that the activation of the caspase cascade could be one of the *in vivo* mechanisms in silibinin-induced apoptotic cell death of prostate tumor.

The reduction in microvessel density in silibinin-fed groups of prostate tumors revealed a novel *in vivo* property of silibinin, the inhibition of tumor angiogenesis, which could have contributed to the inhibition of prostate tumor growth. The observation that silibinin caused a significant decrease in microvessel density (number of microvessels/unit defined area)

[4] Singh, R.P., and Agarwal, R., unpublished data.

could be a biologically important difference because growth of the tumor depends largely on the supply of nutrients and oxygen as well as excretion of the waste metabolic products and CO_2, which are facilitated by the blood vessels. The *in vivo* antiangiogenic effect of silibinin is further supported by a moderate inhibitory effect on VEGF in tumor xenograft and by *in vitro* studies showing inhibition of endothelial cell growth and induction of apoptotic death together with suppression of capillary tube formation on Matrigel assay (19).[4]

Our study supports the argument that silibinin, which inhibits PCA cell growth and has an angiopreventive effect, could be a potential chemopreventive agent for human PCA control. The antiangiogenic effect of silibinin could be helpful in controlling the development of cancer at earlier stages, at which time tumors are latent and localized, before tumors become aggressive and metastatic and require angiogenesis. Furthermore, we would like to mention that in a completed nude mice study, we did not observe any toxicity, which was consistent with earlier reports showing that silibinin and silymarin as well as milk thistle extract (consumed as dietary supplement) are devoid of toxicity. Based on the dose-dependent effect of silibinin on tumor cell proliferation, apoptosis, and angiogenesis, there is a strong possibility that higher doses of silibinin might achieve better and possibly complete PCA growth inhibition. In terms of doses, it should be noted that Neutraceutical Companies suggests up to 2.0 g/day oral consumption of milk thistle extract as a dietary supplement, which corresponds to 0.1% of silibinin on the basis of average food intake in terms of calories. Therefore, PCA xenograft growth inhibition accompanied by the antiproliferative, proapoptotic, and antiangiogenic efficacy of silibinin at dietary dose levels without any noticeable toxicity could have a direct practical and translational relevance to human PCA patients. In this regard, based on our extensive studies with silibinin/silymarin in PCA showing strong efficacy with a mechanistic rationale, we have an ongoing Phase I dose-escalating clinical trial with silibinin in PCA patients.

References

1. Sporn, M. B., and Suh, N. Chemoprevention of cancer. Carcinogenesis (Lond.), *21:* 525–530, 2000.

2. Lippman, S. M., and Hong, W. K. Cancer prevention science and practice. Cancer Res., *62:* 5119–5125, 2002.

3. Clinton, S. K., and Giovannucci, E. Diet, nutrition, and prostate cancer. Annu. Rev. Nutr., *18:* 413–440, 1998.

4. Siess, M. H., Le Bon, A. M., Canivenc, M. C., and Suschetet, M. Mechanisms involved in chemoprevention of flavonoids. Biofactors, *12:* 193–199, 2000.

5. Kelloff, G. J. Perspectives on cancer chemoprevention research and drug development. Adv. Cancer Res., *78:* 199–334, 2000.

6. Vogel, G., Trost, W., and Braatz, R. Studies on the pharmacodynamics, including site and mode of action, of silymarin: the antihepatotoxic principle from *Silybum marianum* (L) Gaertn. Arzneim. Forsch., *25:* 82–89, 1975.

7. Saller, R., Meier, R., and Brignoli, R. The use of silymarin in the treatment of liver diseases. Drugs, *6:* 2035–2063, 2001.

8. Wellington, K., and Jarwis, B. Silymarin: a review of its clinical properties in the management of hepatic disorders. BioDrugs, *15:* 465–489, 2001.

9. Katiyar, S. K., Korman, N. J., Mukhtar, H., and Agarwal, R. Protective effects of silymarin against photocarcinogenesis in a mouse skin model. J. Natl. Cancer Inst. (Bethesda), *89:* 556–566, 1997.

10. Lahiri-Chatterjee, M., Katiyar, S. K., Mohan, R. R., and Agarwal, R. A flavonoid antioxidant, silymarin, affords exceptionally high protection against tumor promotion in SENCAR mouse skin tumorigenesis model. Cancer Res., *59:* 622–632, 1999.

11. Bhatia, N., Zhao, J., Wolf, D. M., and Agarwal, R. Inhibition of human carcinoma cell growth and DNA synthesis by silibinin, an active constituent of milk thistle: comparison with silymarin. Cancer Lett., *147:* 77–84, 1999.

12. Zi, X., and Agarwal, R. Silibinin decreases prostate-specific antigen with cell growth inhibition via G_1 arrest, leading to differentiation of prostate carcinoma cells: implications for prostate cancer intervention. Proc. Natl. Acad. Sci. USA, *96:* 7490–7495, 1999.

13. Singh, R. P., Dhanalakshmi, S., Tyagi, A. K., Chan, D. C. F., Agarwal, C., and Agarwal, R. Dietary feeding of silibinin inhibits advance human prostate carcinoma growth in athymic nude mice, and increases plasma insulin-like growth factor-binding protein-3 levels. Cancer Res., *62:* 3063–3069, 2002.

14. Kish, J. A., Bukkapatnam, R., and Palazzo, F. The treatment challenge of hormone-refractory prostate cancer. Cancer Control, *8:* 487–495, 2001.

15. Carmeliet, P., and Jain, R. K. Angiogenesis in cancer and other diseases. Nat. Med., *407:* 249–257, 2000.

16. Zi, X., Grasso, A. W., Kung, H-J., and Agarwal, R. A flavonoid antioxidant, silymarin, inhibits activation of erbB1 signaling and induces cyclin-dependent kinase inhibitors, G_1 arrest, and anticarcinogenic effects in human prostate carcinoma DU145 cells. Cancer Res., *58:* 1920–1929, 1998.

17. Zi, X., Zhang, J., Agarwal, R., and Pollak, M. Silibinin up-regulates insulin-like growth factor binding protein-3 expression and inhibits proliferation of androgen-independent prostate cancer cells. Cancer Res., *60:* 5617–5620, 2000.

18. Dhanalakshmi, S., Singh, R. P., Agarwal, C., and Agarwal, R. Silibinin inhibits constitutive and TNFα-induced activation of NF-κB and sensitizes human prostate carcinoma DU145 cells to TNFα-induced apoptosis. Oncogene, *21:* 1759–1567, 2002.

19. Jiang, C., Agarwal, R., and Lu, J. Anti-angiogenic potential of a cancer chemopreventive flavonoid antioxidant, silymarin: inhibition of key attributes of vascular endothelial cells and angiogenic cytokine secretion by cancer epithelial cells. Biochem. Biophys. Res. Commun., *276:* 371–378, 2000.

20. Ali, I. U., Senger, D. R., and Smith, L. H. Angiogenesis as a potential biomarker in prostate cancer chemoprevention trials. Urology, *57:* 143–147, 2001.

21. Chan, J. M., Stampfer, M. J., Giovannucci, E., Gann, P. H., Ma, J., Wilkinson, P., Henneken, C. H., and Pollak, M. Plasma insulin-like growth factor-I and prostate cancer risk: a prospective study. Science (Washington DC), *279:* 563–566, 1998.

22. Chokkalingam, A. P., Pollak, M., Fillmore, C-M., Gao, Y-T., Stanczyk, F. Z., Deng, J., Sesterhenn, I. A., Mostofi, F. K., Fears, T. R., Madigan, M. P., Ziegler, R. G., Fraumeni, J. F., and Hsing, A. W. Insulin-like growth factors and prostate cancer: a population-based case-control study in China. Cancer Epidemiol. Biomark. Prev., *10:* 421–427, 2001.

23. Yu, H., and Rohan, T. Role of the insulin-like growth factor family in the cancer development and progression. J. Natl. Cancer Inst. (Bethesda), *92:* 1472–1489, 2000.

Suppression of Advanced Human Prostate Tumor Growth in Athymic Mice by Silibinin Feeding Is Associated with Reduced Cell Proliferation, Increased Apoptosis, and Inhibition of Angiogenesis

Rana P. Singh, Girish Sharma, Sivanandhan Dhanalakshmi, et al.

Updated version	Access the most recent version of this article at: http://cebp.aacrjournals.org/content/12/9/933

Cited articles	This article cites 23 articles, 8 of which you can access for free at: http://cebp.aacrjournals.org/content/12/9/933.full#ref-list-1
Citing articles	This article has been cited by 17 HighWire-hosted articles. Access the articles at: http://cebp.aacrjournals.org/content/12/9/933.full#related-urls

E-mail alerts	Sign up to receive free email-alerts related to this article or journal.
Reprints and Subscriptions	To order reprints of this article or to subscribe to the journal, contact the AACR Publications Department at pubs@aacr.org.
Permissions	To request permission to re-use all or part of this article, use this link http://cebp.aacrjournals.org/content/12/9/933. Click on "Request Permissions" which will take you to the Copyright Clearance Center's (CCC) Rightslink site.